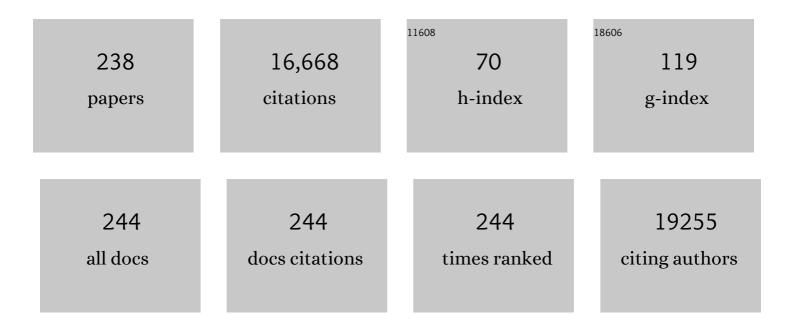
Charles Buddie Mullins

List of Publications by Year in descending order

Source: https://exaly.com/author-pdf/7674517/publications.pdf Version: 2024-02-01



#	Article	IF	CITATIONS
1	Enhancing Visible Light Photo-oxidation of Water with TiO ₂ Nanowire Arrays via Cotreatment with H ₂ and NH ₃ : Synergistic Effects between Ti ³⁺ and N. Journal of the American Chemical Society, 2012, 134, 3659-3662.	6.6	585
2	Amorphous FeOOH Oxygen Evolution Reaction Catalyst for Photoelectrochemical Water Splitting. Journal of the American Chemical Society, 2014, 136, 2843-2850.	6.6	524
3	Visible Light Driven Photoelectrochemical Water Oxidation on Nitrogen-Modified TiO ₂ Nanowires. Nano Letters, 2012, 12, 26-32.	4.5	518
4	Electrode Degradation in Lithium-Ion Batteries. ACS Nano, 2020, 14, 1243-1295.	7.3	484
5	Combined Charge Carrier Transport and Photoelectrochemical Characterization of BiVO ₄ Single Crystals: Intrinsic Behavior of a Complex Metal Oxide. Journal of the American Chemical Society, 2013, 135, 11389-11396.	6.6	435
6	Metal-free photocatalysts for hydrogen evolution. Chemical Society Reviews, 2020, 49, 1887-1931.	18.7	374
7	The Role of Anions in Metal Chalcogenide Oxygen Evolution Catalysis: Electrodeposited Thin Films of Nickel Sulfide as "Pre-catalysts― ACS Energy Letters, 2016, 1, 195-201.	8.8	328
8	Beyond Doping and Coating: Prospective Strategies for Stable High-Capacity Layered Ni-Rich Cathodes. ACS Energy Letters, 2020, 5, 1136-1146.	8.8	313
9	Catalyst or Precatalyst? The Effect of Oxidation on Transition Metal Carbide, Pnictide, and Chalcogenide Oxygen Evolution Catalysts. ACS Energy Letters, 2018, 3, 2956-2966.	8.8	309
10	α-Fe ₂ O ₃ Nanorods as Anode Material for Lithium Ion Batteries. Journal of Physical Chemistry Letters, 2011, 2, 2885-2891.	2.1	306
11	Photoelectrochemical Performance of Nanostructured Ti- and Sn-Doped α-Fe ₂ O ₃ Photoanodes. Chemistry of Materials, 2010, 22, 6474-6482.	3.2	266
12	Silicon Nanowire Fabric as a Lithium Ion Battery Electrode Material. Journal of the American Chemical Society, 2011, 133, 20914-20921.	6.6	251
13	Photoelectrochemical Oxidation of Water Using Nanostructured BiVO ₄ Films. Journal of Physical Chemistry C, 2011, 115, 3794-3802.	1.5	230
14	Unravelling Small-Polaron Transport in Metal Oxide Photoelectrodes. Journal of Physical Chemistry Letters, 2016, 7, 471-479.	2.1	224
15	Incorporation of Mo and W into nanostructured BiVO4 films for efficient photoelectrochemical water oxidation. Physical Chemistry Chemical Physics, 2012, 14, 7065.	1.3	211
16	Selective Hydrogen Production from Formic Acid Decomposition on Pd–Au Bimetallic Surfaces. Journal of the American Chemical Society, 2014, 136, 11070-11078.	6.6	208
17	Surface Science Investigations of Oxidative Chemistry on Gold. Accounts of Chemical Research, 2009, 42, 1063-1073.	7.6	206
18	Solution-Grown Germanium Nanowire Anodes for Lithium-Ion Batteries. ACS Applied Materials & Interfaces, 2012, 4, 4658-4664.	4.0	181

#	Article	IF	CITATIONS
19	Simple Synthesis of Nanocrystalline Tin Sulfide/N-Doped Reduced Graphene Oxide Composites as Lithium Ion Battery Anodes. ACS Nano, 2016, 10, 10778-10788.	7.3	178
20	Nanocolumnar Germanium Thin Films as a High-Rate Sodium-Ion Battery Anode Material. Journal of Physical Chemistry C, 2013, 117, 18885-18890.	1.5	175
21	Sn–Cu Nanocomposite Anodes for Rechargeable Sodium-Ion Batteries. ACS Applied Materials & Interfaces, 2013, 5, 8273-8277.	4.0	173
22	Reactive Ballistic Deposition of α-Fe ₂ O ₃ Thin Films for Photoelectrochemical Water Oxidation. ACS Nano, 2010, 4, 1977-1986.	7.3	172
23	Water-Enhanced Low-Temperature CO Oxidation and Isotope Effects on Atomic Oxygen-Covered Au(111). Journal of the American Chemical Society, 2008, 130, 6801-6812.	6.6	171
24	Transition metal-doped Ni-rich layered cathode materials for durable Li-ion batteries. Nature Communications, 2021, 12, 6552.	5.8	167
25	Highly Efficient Photoelectrochemical Water Splitting from Hierarchical WO ₃ /BiVO ₄ Nanoporous Sphere Arrays. Nano Letters, 2017, 17, 8012-8017.	4.5	164
26	Spray Pyrolysis Deposition and Photoelectrochemical Properties of n-Type BiOI Nanoplatelet Thin Films. ACS Nano, 2012, 6, 7712-7722.	7.3	162
27	Improving the Stability of Nanostructured Silicon Thin Film Lithium-Ion Battery Anodes through Their Controlled Oxidation. ACS Nano, 2012, 6, 2506-2516.	7.3	160
28	On the nature of trapping and desorption at high surface temperatures. Theory and experiments for the Ar–Pt(111) system. Journal of Chemical Physics, 1991, 94, 1516-1527.	1.2	158
29	Cryogenic CO Oxidation on TiO2-Supported Gold Nanoclusters Precovered with Atomic Oxygen. Journal of the American Chemical Society, 2003, 125, 2018-2019.	6.6	151
30	Enhanced Activity Promoted by CeO _{<i>x</i>} on a CoO _{<i>x</i>} Electrocatalyst for the Oxygen Evolution Reaction. ACS Catalysis, 2018, 8, 4257-4265.	5.5	151
31	Nanostructured Si _(1-<i>x</i>) Ge _{<i>x</i>} for Tunable Thin Film Lithium-Ion Battery Anodes. ACS Nano, 2013, 7, 2249-2257.	7.3	150
32	Selective Oxidation of Ethanol to Acetaldehyde on Gold. Journal of the American Chemical Society, 2008, 130, 16458-16459.	6.6	141
33	Facet effect on the photoelectrochemical performance of a WO3/BiVO4 heterojunction photoanode. Applied Catalysis B: Environmental, 2019, 245, 227-239.	10.8	141
34	Synthesis of BiVO ₄ nanoflake array films for photoelectrochemical water oxidation. Journal of Materials Chemistry A, 2014, 2, 9371-9379.	5.2	139
35	Nanostructured Bi2S3/WO3 heterojunction films exhibiting enhanced photoelectrochemical performance. Journal of Materials Chemistry A, 2013, 1, 12826.	5.2	134
36	Electrochemical Synthesis and Characterization of p-CuBi ₂ O ₄ Thin Film Photocathodes. Journal of Physical Chemistry C, 2012, 116, 6459-6466.	1.5	133

#	Article	IF	CITATIONS
37	Simple Synthesis of Nanostructured Sn/Nitrogen-Doped Carbon Composite Using Nitrilotriacetic Acid as Lithium Ion Battery Anode. Chemistry of Materials, 2016, 28, 1343-1347.	3.2	122
38	Synthesis of Ta ₃ N ₅ Nanotube Arrays Modified with Electrocatalysts for Photoelectrochemical Water Oxidation. Journal of Physical Chemistry C, 2012, 116, 14541-14550.	1.5	116
39	In Situ Optical Imaging of Sodium Electrodeposition: Effects of Fluoroethylene Carbonate. ACS Energy Letters, 2017, 2, 2051-2057.	8.8	116
40	Surface Chemistry of Methanol on Clean and Atomic Oxygen Pre-Covered Au(111). Journal of Physical Chemistry C, 2008, 112, 5501-5509.	1.5	114
41	Evidence for Molecularly Chemisorbed Oxygen on TiO2Supported Gold Nanoclusters and Au(111). Journal of the American Chemical Society, 2004, 126, 1606-1607.	6.6	108
42	Synthesis and Characterization of CuV ₂ O ₆ and Cu ₂ V ₂ O ₇ : Two Photoanode Candidates for Photoelectrochemical Water Oxidation. Journal of Physical Chemistry C, 2015, 119, 27220-27227.	1.5	107
43	Water Activated by Atomic Oxygen on Au(111) to Oxidize CO at Low Temperatures. Journal of the American Chemical Society, 2006, 128, 6282-6283.	6.6	106
44	Tin-Seeded Silicon Nanowires for High Capacity Li-Ion Batteries. Chemistry of Materials, 2012, 24, 3738-3745.	3.2	106
45	An active nanoporous Ni(Fe) OER electrocatalyst via selective dissolution of Cd in alkaline media. Applied Catalysis B: Environmental, 2018, 225, 1-7.	10.8	104
46	Na 2 Ni 2 TeO 6 : Evaluation as a cathode for sodium battery. Journal of Power Sources, 2013, 243, 817-821.	4.0	95
47	<i>In situ</i> formation of a multicomponent inorganic-rich SEI layer provides a fast charging and high specific energy Li-metal battery. Journal of Materials Chemistry A, 2019, 7, 17782-17789.	5.2	95
48	Interaction of CO with OH on Au(111): HCOO, CO ₃ , and HOCO as Key Intermediates in the Water-Gas Shift Reaction. Journal of Physical Chemistry C, 2009, 113, 19536-19544.	1.5	93
49	Understanding Charge Transport in Carbon Nitride for Enhanced Photocatalytic Solar Fuel Production. Accounts of Chemical Research, 2019, 52, 248-257.	7.6	93
50	Tuning the Intrinsic Properties of Carbon Nitride for High Quantum Yield Photocatalytic Hydrogen Production. Advanced Science, 2018, 5, 1800820.	5.6	92
51	Reaction of CO with Molecularly Chemisorbed Oxygen on TiO2-Supported Gold Nanoclusters. Journal of the American Chemical Society, 2004, 126, 13574-13575.	6.6	91
52	A high-rate germanium-particle slurry cast Li-ion anode with high Coulombic efficiency and long cycle life. Journal of Power Sources, 2013, 238, 123-136.	4.0	90
53	Model studies of heterogeneous catalytic hydrogenation reactions with gold. Chemical Society Reviews, 2013, 42, 5002.	18.7	89
54	Electrodeposition of Ni-doped FeOOH oxygen evolution reaction catalyst for photoelectrochemical water splitting. Journal of Materials Chemistry A, 2014, 2, 14957.	5.2	88

#	Article	IF	CITATIONS
55	Electrochemical Lithiation of Graphene-Supported Silicon and Germanium for Rechargeable Batteries. Journal of Physical Chemistry C, 2012, 116, 11917-11923.	1.5	87
56	Tin–Germanium Alloys as Anode Materials for Sodium-Ion Batteries. ACS Applied Materials & Interfaces, 2014, 6, 15860-15867.	4.0	85
57	Selective Catalytic Oxidation of Ammonia to Nitrogen on Atomic Oxygen Precovered Au(111). Journal of the American Chemical Society, 2006, 128, 9012-9013.	6.6	83
58	Evaluating Electrocatalysts for the Hydrogen Evolution Reaction Using Bipolar Electrode Arrays: Bi- and Trimetallic Combinations of Co, Fe, Ni, Mo, and W. ACS Catalysis, 2014, 4, 1332-1339.	5.5	83
59	Improved Visible Light Harvesting of WO ₃ by Incorporation of Sulfur or Iodine: A Tale of Two Impurities. Chemistry of Materials, 2014, 26, 1670-1677.	3.2	83
60	Morphology Dependence of the Lithium Storage Capability and Rate Performance of Amorphous TiO ₂ Electrodes. Journal of Physical Chemistry C, 2011, 115, 2585-2591.	1.5	82
61	Capacity Degradation Mechanism and Cycling Stability Enhancement of AlF ₃ -Coated Nanorod Gradient Na[Ni _{0.65} Co _{0.08} Mn _{0.27}]O ₂ Cathode for Sodium-Ion Batteries. ACS Nano, 2018, 12, 12912-12922.	7.3	82
62	Hydrogen Adsorption and Absorption with Pd–Au Bimetallic Surfaces. Journal of Physical Chemistry C, 2013, 117, 19535-19543.	1.5	81
63	Recent Developments in Dendrite-Free Lithium-Metal Deposition through Tailoring of Micro- and Nanoscale Artificial Coatings. ACS Nano, 2021, 15, 29-46.	7.3	80
64	Influences of Gold, Binder and Electrolyte on Silicon Nanowire Performance in Li-Ion Batteries. Journal of Physical Chemistry C, 2012, 116, 18079-18086.	1.5	79
65	p-Si/W ₂ C and p-Si/W ₂ C/Pt Photocathodes for the Hydrogen Evolution Reaction. Journal of the American Chemical Society, 2014, 136, 1535-1544.	6.6	77
66	Ethanol Decomposition on Pd–Au Alloy Catalysts. Journal of Physical Chemistry C, 2018, 122, 22024-22032.	1.5	77
67	Nanostructured Ta ₃ N ₅ Films as Visible-Light Active Photoanodes for Water Oxidation. Journal of Physical Chemistry C, 2012, 116, 19225-19232.	1.5	76
68	Anisotropic small-polaron hopping in W:BiVO4 single crystals. Applied Physics Letters, 2015, 106, .	1.5	75
69	Screening of transition and post-transition metals to incorporate into copper oxide and copper bismuth oxide for photoelectrochemical hydrogen evolution. Physical Chemistry Chemical Physics, 2013, 15, 4554.	1.3	74
70	Highâ€Rate Oxygen Evolution Reaction on Alâ€Doped LiNiO ₂ . Advanced Materials, 2015, 27, 6063-6067.	11.1	74
71	K ⁺ Reduces Lithium Dendrite Growth by Forming a Thin, Less-Resistive Solid Electrolyte Interphase. ACS Energy Letters, 2016, 1, 414-419.	8.8	72
72	Tantalum Cobalt Nitride Photocatalysts for Water Oxidation under Visible Light. Chemistry of Materials, 2012, 24, 579-586.	3.2	71

#	Article	IF	CITATIONS
73	Effect of Si Doping and Porosity on Hematite's (α-Fe ₂ O ₃) Photoelectrochemical Water Oxidation Performance. Journal of Physical Chemistry C, 2012, 116, 5255-5261.	1.5	70
74	SnO2 and TiO2-supported-SnO2 lithium battery anodes with improved electrochemical performance. Journal of Materials Chemistry, 2012, 22, 11134.	6.7	70
75	Optimum lithium-ion conductivity in cubic Li7â^'xLa3Hf2â^'xTaxO12. Journal of Power Sources, 2012, 209, 184-188.	4.0	70
76	Parallel Screening of Electrocatalyst Candidates Using Bipolar Electrochemistry. Analytical Chemistry, 2013, 85, 2493-2499.	3.2	70
77	Selective Oxidation of Propanol on Au(111): Mechanistic Insights into Aerobic Oxidation of Alcohols. ChemPhysChem, 2008, 9, 2461-2466.	1.0	67
78	Coincorporation of N and Ta into TiO ₂ Nanowires for Visible Light Driven Photoelectrochemical Water Oxidation. Journal of Physical Chemistry C, 2012, 116, 23283-23290.	1.5	64
79	Antimony-Doped Tin Oxide Nanorods as a Transparent Conducting Electrode for Enhancing Photoelectrochemical Oxidation of Water by Hematite. ACS Applied Materials & Interfaces, 2014, 6, 5494-5499.	4.0	63
80	Highly active and stable nickel–molybdenum nitride (Ni ₂ Mo ₃ N) electrocatalyst for hydrogen evolution. Journal of Materials Chemistry A, 2021, 9, 4945-4951.	5.2	60
81	Facile Synthesis of Ge/N-Doped Carbon Spheres with Varying Nitrogen Content for Lithium Ion Battery Anodes. ACS Applied Materials & Interfaces, 2016, 8, 27788-27794.	4.0	59
82	Mechanism for the water–gas shift reaction on monofunctional platinum and cause of catalyst deactivation. Journal of Catalysis, 2011, 282, 278-288.	3.1	58
83	Carbon Nitride Transforms into a High Lithium Storage Capacity Nitrogen-Rich Carbon. ACS Nano, 2019, 13, 9279-9291.	7.3	58
84	Adsorption and Reaction of Nitric Oxide with Atomic Oxygen Covered Au(111). Journal of Physical Chemistry B, 2004, 108, 17952-17958.	1.2	57
85	Low-Temperature Hydrogenation of Acetaldehyde to Ethanol on H-Precovered Au(111). Journal of Physical Chemistry Letters, 2011, 2, 1363-1367.	2.1	57
86	Oxygen Activation and Reaction on Pd–Au Bimetallic Surfaces. Journal of Physical Chemistry C, 2015, 119, 11754-11762.	1.5	57
87	Mechanistic insights on ethanol dehydrogenation on Pd–Au model catalysts: a combined experimental and DFT study. Physical Chemistry Chemical Physics, 2017, 19, 30578-30589.	1.3	57
88	Reactive Ballistic Deposition of Porous TiO2Films:  Growth and Characterization. Journal of Physical Chemistry C, 2007, 111, 4765-4773.	1.5	56
89	Modulating Charge Transfer Efficiency of Hematite Photoanode with Hybrid Dualâ€Metal–Organic Frameworks for Boosting Photoelectrochemical Water Oxidation. Advanced Science, 2020, 7, 2002563.	5.6	56
90	Selective decomposition of formic acid on molybdenum carbide: A new reaction pathway. Journal of Catalysis, 2010, 269, 33-43.	3.1	55

#	Article	IF	CITATIONS
91	Low Temperature Synthesis and Characterization of Nanocrystalline Titanium Carbide with Tunable Porous Architectures. Chemistry of Materials, 2010, 22, 319-329.	3.2	54
92	Interface Engineering and its Effect on WO ₃ -Based Photoanode and Tandem Cell. ACS Applied Materials & Interfaces, 2018, 10, 12639-12650.	4.0	54
93	Solvent-free vacuum growth of oriented HKUST-1 thin films. Journal of Materials Chemistry A, 2019, 7, 19396-19406.	5.2	54
94	Anodized Nickel Foam for Oxygen Evolution Reaction in Fe-Free and Unpurified Alkaline Electrolytes at High Current Densities. ACS Nano, 2021, 15, 3468-3480.	7.3	54
95	Storage of Lithium in Hydrothermally Synthesized GeO ₂ Nanoparticles. Journal of Physical Chemistry Letters, 2013, 4, 999-1004.	2.1	53
96	High tap density microparticles of selenium-doped germanium as a high efficiency, stable cycling lithium-ion battery anode material. Journal of Materials Chemistry A, 2015, 3, 5829-5834.	5.2	52
97	Activation of a Nickel-Based Oxygen Evolution Reaction Catalyst on a Hematite Photoanode via Incorporation of Cerium for Photoelectrochemical Water Oxidation. ACS Applied Materials & Interfaces, 2017, 9, 30654-30661.	4.0	52
98	n-BiSI Thin Films: Selenium Doping and Solar Cell Behavior. Journal of Physical Chemistry C, 2012, 116, 24878-24886.	1.5	51
99	BiSI Micro-Rod Thin Films: Efficient Solar Absorber Electrodes?. Journal of Physical Chemistry Letters, 2012, 3, 1571-1576.	2.1	51
100	Mechanisms of Initial Dissociative Chemisorption of Oxygen on Transition-Metal Surfaces. Accounts of Chemical Research, 1998, 31, 798-804.	7.6	50
101	Probing the Degradation Chemistry and Enhanced Stability of 2D Organolead Halide Perovskites. Journal of the American Chemical Society, 2019, 141, 18170-18181.	6.6	50
102	Stabilization of a Highly Ni-Rich Layered Oxide Cathode through Flower-Petal Grain Arrays. ACS Nano, 2020, 14, 17142-17150.	7.3	50
103	Pulsed Laser Deposition of Epitaxial and Polycrystalline Bismuth Vanadate Thin Films. Journal of Physical Chemistry C, 2014, 118, 26543-26550.	1.5	49
104	Facile growth of porous Fe ₂ V ₄ O ₁₃ films for photoelectrochemical water oxidation. Journal of Materials Chemistry A, 2016, 4, 3034-3042.	5.2	49
105	Surface Alloy Composition Controlled O ₂ Activation on Pd–Au Bimetallic Model Catalysts. ACS Catalysis, 2018, 8, 3641-3649.	5.5	49
106	Mass transport-enhanced electrodeposition of Ni–S–P–O films on nickel foam for electrochemical water splitting. Journal of Materials Chemistry A, 2021, 9, 7736-7749.	5.2	49
107	Growth and Characterization of High Surface Area Titanium Carbide. Journal of Physical Chemistry C, 2009, 113, 12742-12752.	1.5	48
108	Li- and Na-reduction products of meso-Co ₃ O ₄ form high-rate, stably cycling battery anode materials. Journal of Materials Chemistry A, 2014, 2, 14209-14221.	5.2	48

#	Article	IF	CITATIONS
109	Development of a chlorine mechanism for use in the carbon bond IV chemistry model. Journal of Geophysical Research, 2003, 108, .	3.3	45
110	CO oxidation on inverse Fe2O3/Au(111) model catalysts. Journal of Catalysis, 2012, 294, 216-222.	3.1	45
111	Electrodeposition of MoS _{<i>x</i>} Hydrogen Evolution Catalysts from Sulfur-Rich Precursors. ACS Applied Materials & Interfaces, 2019, 11, 32879-32886.	4.0	45
112	Nanorod Gradient Cathode: Preventing Electrolyte Penetration into Cathode Particles. ACS Applied Energy Materials, 2019, 2, 6002-6011.	2.5	45
113	The effect of local lithium surface chemistry and topography on solid electrolyte interphase composition and dendrite nucleation. Journal of Materials Chemistry A, 2019, 7, 14882-14894.	5.2	45
114	A Perspective on the Electrochemical Oxidation of Methane to Methanol in Membrane Electrode Assemblies. ACS Energy Letters, 2020, 5, 2954-2963.	8.8	45
115	Low temperature CO oxidation on Au(111) and the role of adsorbed water. Topics in Catalysis, 2007, 44, 57-63.	1.3	44
116	Tin microparticles for a lithium ion battery anode with enhanced cycling stability and efficiency derived from Se-doping. Journal of Materials Chemistry A, 2015, 3, 13500-13506.	5.2	42
117	In Situ Growth of Fe(Ni)OOH Catalyst on Stainless Steel for Water Oxidation. ChemistrySelect, 2017, 2, 2230-2234.	0.7	42
118	Lithium Fluoride Coated Silicon Nanocolumns as Anodes for Lithium Ion Batteries. ACS Applied Materials & Interfaces, 2020, 12, 18465-18472.	4.0	41
119	Carbonate Formation and Decomposition on Atomic Oxygen Precovered Au(111). Journal of the American Chemical Society, 2008, 130, 11250-11251.	6.6	39
120	Structural and Catalytic Effects of Iron- and Scandium-Doping on a Strontium Cobalt Oxide Electrocatalyst for Water Oxidation. ACS Catalysis, 2016, 6, 1122-1133.	5.5	39
121	Evidence that Amorphous Water below 160 K Is Not a Fragile Liquid. Journal of Physical Chemistry B, 2006, 110, 11033-11036.	1.2	38
122	Chemical bath deposition of vertically aligned TiO2 nanoplatelet arrays for solar energy conversion applications. Journal of Materials Chemistry A, 2013, 1, 4307.	5.2	38
123	Sulfur-Rich MoS ₆ as an Electrocatalyst for the Hydrogen Evolution Reaction. ACS Applied Energy Materials, 2018, 1, 4453-4458.	2.5	38
124	Reactive Scattering of CO from an Oxygen-Atom-Covered Au/TiO2Model Catalyst. Journal of Physical Chemistry B, 2004, 108, 7917-7926.	1.2	37
125	Oxygen and Hydroxyl Species Induce Multiple Reaction Pathways for the Partial Oxidation of Allyl Alcohol on Gold. Journal of the American Chemical Society, 2014, 136, 6489-6498.	6.6	37
126	Reactive Ballistic Deposition of Nanostructured Model Materials for Electrochemical Energy Conversion and Storage. Accounts of Chemical Research, 2012, 45, 434-443.	7.6	36

#	Article	IF	CITATIONS
127	Self-Assembled Cu–Sn–S Nanotubes with High (De)Lithiation Performance. ACS Nano, 2017, 11, 10347-10356.	7.3	35
128	Transport in Amorphous Solid Water Films:Â Implications for Self-Diffusivity. Journal of Physical Chemistry B, 2006, 110, 17987-17997.	1.2	34
129	Structure Revealing H/D Exchange with Co-Adsorbed Hydrogen and Water on Gold. Journal of Physical Chemistry Letters, 2012, 3, 1894-1899.	2.1	34
130	Oxygen Exchange in the Selective Oxidation of 2-Butanol on Oxygen Precovered Au(111). Journal of the American Chemical Society, 2009, 131, 16189-16194.	6.6	32
131	Model Studies with Gold: A Versatile Oxidation and Hydrogenation Catalyst. Accounts of Chemical Research, 2014, 47, 750-760.	7.6	32
132	SILAR Growth of Ag ₃ VO ₄ and Characterization for Photoelectrochemical Water Oxidation. Journal of Physical Chemistry C, 2015, 119, 26803-26808.	1.5	32
133	Cobalt Metal–Cobalt Carbide Composite Microspheres for Water Reduction Electrocatalysis. ACS Applied Energy Materials, 2020, 3, 3909-3918.	2.5	32
134	Hydrogen Evolution by Ni ₂ P Catalysts Derived from Phosphine MOFs. ACS Applied Energy Materials, 2020, 3, 176-183.	2.5	31
135	Water Influences the Activity and Selectivity of Ceria-Supported Gold Catalysts for Oxidative Dehydrogenation and Esterification of Ethanol. ACS Catalysis, 2017, 7, 1216-1226.	5.5	30
136	Effect of the Electrolyte on the Cycling Efficiency of Lithium-Limited Cells and their Morphology Studied Through in Situ Optical Imaging. ACS Applied Energy Materials, 2018, 1, 5830-5835.	2.5	30
137	NiAl2O4 as a beneficial precursor for Ni/Al2O3 catalysts for the dry reforming of methane. Journal of CO2 Utilization, 2022, 63, 102112.	3.3	30
138	Hybrid Generalized Ellipsometry and Quartz Crystal Microbalance Nanogravimetry for the Determination of Adsorption Isotherms on Biaxial Metal Oxide Films. Journal of Physical Chemistry Letters, 2010, 1, 1264-1268.	2.1	29
139	The Effects of Adsorbed Water on Gold Catalysis and Surface Chemistry. Topics in Catalysis, 2013, 56, 1499-1511.	1.3	29
140	Atomic layer deposition of photoactive CoO/SrTiO3 and CoO/TiO2 on Si(001) for visible light driven photoelectrochemical water oxidation. Journal of Applied Physics, 2013, 114, .	1.1	29
141	The Effect of Adsorbed Water in CO Oxidation on Au/TiO ₂ (110). Journal of Physical Chemistry C, 2011, 115, 2057-2065.	1.5	28
142	p-Type BP nanosheet photocatalyst with AQE of 3.9% in the absence of a noble metal cocatalyst: investigation and elucidation of photophysical properties. Journal of Materials Chemistry A, 2018, 6, 18403-18408.	5.2	28
143	Oxidative Cross-Esterification and Related Pathways of Co-Adsorbed Oxygen and Ethanol on Pd–Au. ACS Catalysis, 2019, 9, 4516-4525.	5.5	28
144	Boosting Photoelectrochemical Performance of BiVO ₄ through Photoassisted Self-Reduction. ACS Applied Energy Materials, 2020, 3, 4403-4410.	2.5	28

#	Article	IF	CITATIONS
145	Electrochemical behavior of a Ni ₃ N OER precatalyst in Fe-purified alkaline media: the impact of self-oxidation and Fe incorporation. Materials Advances, 2021, 2, 2299-2309.	2.6	28
146	Lithium Insertion/Deinsertion Characteristics of Nanostructured Amorphous Tantalum Oxide Thin Films. ChemElectroChem, 2014, 1, 158-164.	1.7	27
147	Bandgap engineering of Fe ₂ O ₃ with Cr – application to photoelectrochemical oxidation. Physical Chemistry Chemical Physics, 2016, 18, 1644-1648.	1.3	27
148	Sub-stoichiometric germanium sulfide thin-films as a high-rate lithium storage material. Journal of Materials Chemistry A, 2014, 2, 19011-19018.	5.2	26
149	Synthesis, electronic transport and optical properties of Si:α-Fe ₂ O ₃ single crystals. Journal of Materials Chemistry C, 2016, 4, 559-567.	2.7	26
150	Reduced-Graphene Oxide/Poly(acrylic acid) Aerogels as a Three-Dimensional Replacement for Metal-Foil Current Collectors in Lithium-Ion Batteries. ACS Applied Materials & Interfaces, 2017, 9, 22641-22651.	4.0	26
151	Cu ₄ SnS ₄ -Rich Nanomaterials for Thin-Film Lithium Batteries with Enhanced Conversion Reaction. ACS Nano, 2019, 13, 10671-10681.	7.3	26
152	Selective Oxidation of Acetaldehyde to Acetic Acid on Pd–Au Bimetallic Model Catalysts. ACS Catalysis, 2019, 9, 4360-4368.	5.5	26
153	Fast lithium transport in PbTe for lithium-ion battery anodes. Journal of Materials Chemistry A, 2014, 2, 7238.	5.2	25
154	NH ₃ -assisted chloride flux-coating method for direct fabrication of visible-light-responsive SrNbO ₂ N crystal layers. CrystEngComm, 2017, 19, 5532-5541.	1.3	25
155	Methanol Oxidation Catalyzed by Copper Nanoclusters Incorporated in Vacuum-Deposited HKUST-1 Thin Films. ACS Catalysis, 2020, 10, 4997-5007.	5.5	25
156	Visible-Light-Active NiV ₂ O ₆ Films for Photoelectrochemical Water Oxidation. Journal of Physical Chemistry C, 2015, 119, 14524-14531.	1.5	24
157	Phase transition systematics in <mml:math xmlns:mml="http://www.w3.org/1998/Math/MathML"><mml:msub><mml:mi>BiVO</mml:mi><mml:mn>4by means of high-pressure–high-temperature Raman experiments. Physical Review B, 2018, 98, .</mml:mn></mml:msub></mml:math 	l:mn♪ <td>ml:മങ്കub></td>	ml:മങ്കub>
158	Reactivity of Molecularly Chemisorbed Oxygen on a Au/TiO2Model Catalyst. Journal of Physical Chemistry B, 2006, 110, 20337-20343.	1.2	23
159	Effect of annealing in oxygen on alloy structures of Pd–Au bimetallic model catalysts. Physical Chemistry Chemical Physics, 2015, 17, 20588-20596.	1.3	23
160	Enhanced Electrochemical Performance of a Tinâ^'antimony Alloy/Nâ€Doped Carbon Nanocomposite as a Sodiumâ€ion Battery Anode. ChemElectroChem, 2018, 5, 391-396.	1.7	23
161	Separator-free and concentrated LiNO ₃ electrolyte cells enable uniform lithium electrodeposition. Journal of Materials Chemistry A, 2020, 8, 3999-4006.	5.2	23
162	Formation of Molecularly Chemisorbed Oxygen on TiO2-Supported Gold Nanoclusters and Au(111) from Exposure to an Oxygen Plasma Jet. Journal of Physical Chemistry B, 2005, 109, 6316-6322.	1.2	22

#	Article	IF	CITATIONS
163	Control of selectivity in allylic alcohol oxidation on gold surfaces: the role of oxygen adatoms and hydroxyl species. Physical Chemistry Chemical Physics, 2015, 17, 4730-4738.	1.3	22
164	Catalytic Reactions on Pd–Au Bimetallic Model Catalysts. Accounts of Chemical Research, 2021, 54, 379-387.	7.6	22
165	<i>In situ</i> and <i>operando</i> investigation of the dynamic morphological and phase changes of a selenium-doped germanium electrode during (de)lithiation processes. Journal of Materials Chemistry A, 2020, 8, 750-759.	5.2	21
166	Evaluation of Two Potassium-Based Activation Agents for the Production of Oxygen- and Nitrogen-Doped Porous Carbons. Energy & Fuels, 2020, 34, 6101-6112.	2.5	21
167	Transformation of a Cobalt Carbide (Co ₃ C) Oxygen Evolution Precatalyst. ACS Applied Energy Materials, 0, , .	2.5	20
168	Facile Synthesis of a Tin Oxide-Carbon Composite Lithium-Ion Battery Anode with High Capacity Retention. ACS Applied Energy Materials, 2019, 2, 7244-7255.	2.5	20
169	Influence of Hydrofluoric Acid Formation on Lithium Ion Insertion in Nanostructured V ₂ O ₅ . Journal of Physical Chemistry C, 2012, 116, 21208-21215.	1.5	19
170	Thin Nanocolumnar Ge _{0.9} Se _{0.1} Films Are Rapidly Lithiated/Delithiated. Journal of Physical Chemistry C, 2014, 118, 17407-17412.	1.5	19
171	Tunable Syn-gas ratio via bireforming over coke-resistant Ni/Mo2C catalyst. Fuel Processing Technology, 2016, 153, 111-120.	3.7	19
172	CaCl ₂ -Activated Carbon Nitride: Hierarchically Nanoporous Carbons with Ultrahigh Nitrogen Content for Selective CO ₂ Adsorption. ACS Applied Nano Materials, 2020, 3, 5965-5977.	2.4	19
173	Li–Zn Overlayer to Facilitate Uniform Lithium Deposition for Lithium Metal Batteries. ACS Applied Materials & Interfaces, 2021, 13, 9985-9993.	4.0	19
174	Annealing Effect on Reactivity of Oxygen-Covered Au(111). Journal of Physical Chemistry C, 2009, 113, 9820-9825.	1.5	18
175	One-step waferscale synthesis of 3-D ZnO nanosuperstructures by designed catalysts for substantial improvement of solar water oxidation efficiency. Journal of Materials Chemistry A, 2013, 1, 8111.	5.2	18
176	Lead Oxide Microparticles Coated by Ethylenediamine-Cross-Linked Graphene Oxide for Lithium Ion Battery Anodes. ACS Applied Energy Materials, 2019, 2, 3017-3020.	2.5	18
177	Simultaneous Sulfite Electrolysis and Hydrogen Production Using Ni Foam-Based Three-Dimensional Electrodes. Environmental Science & Technology, 2020, 54, 12511-12520.	4.6	18
178	Investigation of 35 Elements as Single Metal Oxides, Mixed Metal Oxides, or Dopants for Titanium Dioxide for Dye-Sensitized Solar Cells. Journal of Physical Chemistry C, 2013, 117, 25248-25258.	1.5	17
179	Interactions of Hydrogen and Carbon Monoxide on Pd–Au Bimetallic Surfaces. Journal of Physical Chemistry C, 2014, 118, 2129-2137.	1.5	17
180	Improved Charge Carrier Transport of Hydrogen-Treated Copper Tungstate: Photoelectrochemical and Computational Study. Journal of the Electrochemical Society, 2016, 163, H970-H975.	1.3	17

#	Article	IF	CITATIONS
181	A Simplified Successive Ionic Layer Adsorption and Reaction (s-SILAR) Method for Growth of Porous BiVO ₄ Thin Films for Photoelectrochemical Water Oxidation. Journal of the Electrochemical Society, 2017, 164, H119-H125.	1.3	17
182	Effect of Selenium Content on Nickel Sulfoselenide-Derived Nickel (Oxy)hydroxide Electrocatalysts for Water Oxidation. ACS Applied Materials & Interfaces, 2020, 12, 20366-20375.	4.0	17
183	Calcium Poly(Heptazine Imide): A Covalent Heptazine Framework for Selective CO ₂ Adsorption. ACS Nano, 2022, 16, 5393-5403.	7.3	17
184	Lithiation and Delithiation of Lead Sulfide (PbS). Journal of the Electrochemical Society, 2015, 162, A1182-A1185.	1.3	16
185	A soft X-ray spectroscopic perspective of electron localization and transport in tungsten doped bismuth vanadate single crystals. Physical Chemistry Chemical Physics, 2016, 18, 31958-31965.	1.3	16
186	In Situ Focused Ion Beam-Scanning Electron Microscope Study of Crack and Nanopore Formation in Germanium Particle During (De)lithiation. ACS Applied Energy Materials, 2019, 2, 2441-2446.	2.5	16
187	Current Progress and Future Directions in Gasâ€Phase Metalâ€Organic Framework Thinâ€Film Growth. ChemSusChem, 2020, 13, 5433-5442.	3.6	16
188	Interaction of water with the clean and oxygen pre-covered Ir(111) surfaceâ~†. Catalysis Today, 2011, 160, 198-203.	2.2	15
189	Communication—Stages in the Dynamic Electrochemical Lithiation of Lead. Journal of the Electrochemical Society, 2016, 163, A1027-A1029.	1.3	15
190	Enhanced Photoelectrochemical Performance of Porous Bi ₂ MoO ₆ Photoanode by an Electrochemical Treatment. Journal of the Electrochemical Society, 2017, 164, H299-H306.	1.3	15
191	The interplay between ceria particle size, reducibility, and ethanol oxidation activity of ceria-supported gold catalysts. Reaction Chemistry and Engineering, 2018, 3, 75-85.	1.9	15
192	Simple Microwaveâ€Assisted Synthesis of Delafossite CuFeO 2 as an Anode Material for Sodiumâ€Ion Batteries. ChemElectroChem, 2018, 5, 2419-2423.	1.7	15
193	Sulfur-Rich Molybdenum Sulfide as a Cathode Material for Room Temperature Sodium–Sulfur Batteries. ACS Applied Energy Materials, 2020, 3, 6121-6126.	2.5	15
194	Methanol O–H Bond Dissociation on H-Precovered Gold Originating from a Structure with a Wide Range of Surface Stability. Journal of Physical Chemistry C, 2012, 116, 20982-20989.	1.5	13
195	An environmental chamber investigation of chlorine-enhanced ozone formation in Houston, Texas. Journal of Geophysical Research, 2003, 108, .	3.3	12
196	Oxygen-Electrode Catalysis on Oxoperovskites at 700 °C versus 20 °C. Chemistry of Materials, 2018, 30, 629-635.	3.2	12
197	Enhanced Carbonate Formation on Gold. Journal of Physical Chemistry C, 2008, 112, 17631-17634.	1.5	11
198	Lowâ€Temperature Chemoselective Goldâ€Surfaceâ€Mediated Hydrogenation of Acetone and Propionaldehyde. ChemCatChem, 2012, 4, 1241-1244.	1.8	11

#	Article	IF	CITATIONS
199	Improvement of Solar Energy Conversion with Nbâ€Incorporated TiO ₂ Hierarchical Microspheres. ChemPhysChem, 2013, 14, 2270-2276.	1.0	11
200	Water's place in Au catalysis. Science, 2014, 345, 1564-1565.	6.0	11
201	Controlled Prelithiation of PbS to Pb/Li ₂ S for High Initial Coulombic Efficiency in Lithium Ion Batteries. Journal of the Electrochemical Society, 2019, 166, A1939-A1943.	1.3	11
202	Electrodeposition of the NaK Alloy with a Liquid Organic Electrolyte. ACS Applied Energy Materials, 2019, 2, 3009-3012.	2.5	11
203	Moisture-Driven Formation and Growth of Quasi-2-D Organolead Halide Perovskite Crystallites. ACS Applied Energy Materials, 2020, 3, 6280-6290.	2.5	11
204	Highly Selective, Facile NO ₂ Reduction to NO at Cryogenic Temperatures on Hydrogen Precovered Gold. Journal of the American Chemical Society, 2013, 135, 436-442.	6.6	10
205	Investigation of Reversible Li Insertion into LiY(WO ₄) ₂ . Chemistry of Materials, 2016, 28, 4641-4645.	3.2	10
206	Formation of an Electroactive Polymer Gel Film upon Lithiation and Delithiation of PbSe. Journal of the Electrochemical Society, 2016, 163, A1666-A1671.	1.3	10
207	Inâ€Situ Characterization of Dynamic Morphological and Phase Changes of Seleniumâ€doped Germanium Using a Single Particle Cell and Synchrotron Transmission Xâ€ray Microscopy. ChemSusChem, 2021, 14, 1370-1376.	3.6	10
208	Tunable Ether Production via Coupling of Aldehydes or Aldehyde/Alcohol over Hydrogen-Modified Gold Catalysts at Low Temperatures. Journal of Physical Chemistry Letters, 2012, 3, 2512-2516.	2.1	9
209	Mixing Super P-Li with N-Doped Mesoporous Templated Carbon Improves the High Rate Performance of a Potential Lithium Ion Battery Anode. Journal of the Electrochemical Society, 2016, 163, A953-A957.	1.3	9
210	Apparatus for efficient utilization of isotopically-labeled gases in pulse transient studies of heterogeneously catalyzed gas phase reactions. Reaction Chemistry and Engineering, 2017, 2, 512-520.	1.9	9
211	Compact Lithium-Ion Battery Electrodes with Lightweight Reduced Graphene Oxide/Poly(Acrylic Acid) Current Collectors. ACS Applied Energy Materials, 2019, 2, 905-912.	2.5	9
212	Surface Chemistry of 2-Propanol on Clean and Oxygen Precovered Ir(111). Journal of Physical Chemistry C, 2009, 113, 21745-21754.	1.5	8
213	Electrochemical probings of Li1+xVS2. Electrochimica Acta, 2012, 78, 430-433.	2.6	8
214	Chloride Flux Growth of Idiomorphic <i>A</i> WO ₄ (<i>A</i> = Sr, Ba) Single Microcrystals. Crystal Growth and Design, 2018, 18, 5301-5310.	1.4	8
215	In Situ and Operando Morphology Study of Germanium–Selenium Alloy Anode for Lithium-Ion Batteries. ACS Applied Energy Materials, 2020, 3, 6115-6120.	2.5	8
216	Effect of Dilute Nitric Acid on Crystallization and Fracture of Amorphous Solid Water Films. Journal of Physical Chemistry C, 2007, 111, 10438-10447.	1.5	7

#	Article	IF	CITATIONS
217	A free-standing, flexible lithium-ion anode formed from an air-dried slurry cast of high tap density SnO ₂ , CMC polymer binder and Super-P Li. Journal of Materials Chemistry A, 2014, 2, 14459.	5.2	7
218	Obviating the need for nanocrystallites in the extended lithiation/de-lithiation of germanium. Journal of Materials Chemistry A, 2015, 3, 23442-23447.	5.2	7
219	A Stable Lead (II) Oxide-Carbon Composite Anode Candidate for Secondary Lithium Batteries. Journal of the Electrochemical Society, 2020, 167, 060509.	1.3	7
220	Blade-Type Reaction Front in Micrometer-Sized Germanium Particles during Lithiation. ACS Applied Materials & Interfaces, 2020, 12, 47574-47579.	4.0	7
221	Hydrogen desorption from the surface and subsurface of cobalt. Physical Chemistry Chemical Physics, 2020, 22, 15281-15287.	1.3	7
222	Effects of Alkylammonium Choice on Stability and Performance of Quasi-2D Organolead Halide Perovskites. Journal of Physical Chemistry C, 2020, 124, 10887-10897.	1.5	7
223	Taking a Selective Bite Out of Methane. Science, 2008, 319, 736-737.	6.0	6
224	H ₂ O-Improved O ₂ activation on the Pd–Au bimetallic surface. Chemical Communications, 2017, 53, 3990-3993.	2.2	6
225	Infrared Light-Driven LaW(O,N) ₃ OER Photoelectrocatalysts from Chloride Flux-Grown La ₄ W ₃ O ₁₅ Templating Precursors. ACS Applied Energy Materials, 2019, 2, 913-922.	2.5	6
226	Evaluation of a V ₈ C ₇ Anode for Oxygen Evolution in Alkaline Media: Unusual Morphological Behavior. ACS Sustainable Chemistry and Engineering, 2020, 8, 14101-14108.	3.2	6
227	Improvement of the sodiation/de-sodiation stability of Sn(C) by electrochemically inactive Na ₂ Se. RSC Advances, 2015, 5, 82012-82017.	1.7	5
228	Heterogeneity in Mixed Cerium Oxides and Its Influence on the Behavior of Gold Catalysts for the Selective Oxidation of Ethanol. Journal of Physical Chemistry C, 2017, 121, 19269-19279.	1.5	5
229	Spatially Controlled Molecular Analysis of Biological Samples Using Nanodroplet Arrays and Direct Droplet Aspiration. Journal of the American Society for Mass Spectrometry, 2020, 31, 418-428.	1.2	5
230	Unraveling porogenesis in nitrogen rich K+-activated carbons. Carbon, 2022, 186, 711-723.	5.4	5
231	Understanding the Mechanism of Stress Mitigation in Selenium-Doped Germanium Electrodes. Journal of the Electrochemical Society, 2019, 166, A364-A377.	1.3	4
232	Sulfurâ€Rich Molybdenum Sulfide as an Anode Coating to Improve Performance of Lithium Metal Batteries. ChemElectroChem, 2020, 7, 222-228.	1.7	4
233	Conditions for Ta ^{IV} –Ta ^{IV} Bonding in Trirutile Li _{<i>x</i>} <i>M</i> Ta ₂ O ₆ . Inorganic Chemistry, 2015, 54, 2009-2016.	1.9	3
234	Evidence of methane adsorption over Mo ₂ C involving single C–H bond dissociation instead of facile carbon exchange. Reaction Chemistry and Engineering, 2016, 1, 667-674.	1.9	3

#	Article	IF	CITATIONS
235	CO Dissociation on model Co/SiO2 catalysts – effect of adsorbed hydrogen. Surface Science, 2021, 705, 121783.	0.8	3
236	Low temperature dissociation of CO on manganese promoted cobalt(poly). Chemical Communications, 2020, 56, 2865-2868.	2.2	2
237	A phase transition-induced photocathodic p-CuFeO2 nanocolumnar film by reactive ballistic deposition. New Journal of Chemistry, 2022, 46, 1238-1245.	1.4	2
238	Lithium trapping in germanium nanopores during delithiation process. Applied Materials Today, 2021, 24, 101140.	2.3	1